Overlap parameters of H_2-H_2 molecular pairs from the absorption spectra of the collision-induced fundamental band of H_2†

S. Paddi Reddy, G. Varghese,* and R. D. G. Prasad‡
Department of Physics, Memorial University of Newfoundland, St. John's, Newfoundland, Canada A1C 5S7
(Received 11 August 1976)

The collision-induced fundamental infrared absorption band of H_2 in the pure gas at 77, 196, and 298 K was recorded for a number of gas densities up to 60 amagat. An analysis of the absorption profiles was performed by assuming appropriate line shapes, and the characteristic half-width parameters δ_d and δ_c of the short-range overlap-induced transitions and δ_q (and δ_q') of the long-range quadrupole-induced transitions were determined. From this analysis the contributions to the intensity of the band from the overlap and quadrupolar interactions were separated. For the H_2-H_2 molecular pairs, the overlap parameters, λ and ρ, which give, respectively, the magnitude and range of the overlap dipole moment, and $\mu(\sigma)$, the overlap-induced dipole moment at the Lennard-Jones intermolecular diameter σ, were determined by obtaining the best fit of the calculated overlap parts of the binary absorption coefficients as a function of temperature to the experimental values. The values of the overlap parameters obtained are $\lambda = 4.53 \times 10^{-3}$, $\rho = 0.23$ Å, and $\mu(\sigma) = 2.5 \times 10^{-2} e a_0$.

I. INTRODUCTION

Since the first observation of the collision-induced absorption of the fundamental band of H_2,[1] there have been extensive studies of the collision-induced spectra of H_2 under a variety of experimental conditions.[2-4] According to the theory of the collision-induced absorption,[5,6] the dipole moment induced in a pair of colliding molecules is represented by the so-called "exponential-4" model and the interaction potential is represented by the Lennard-Jones intermolecular potential. In this model the induced dipole moment consists of two additive parts: One part is the isotropic short-range overlap moment, which decreases exponentially with increasing intermolecular separation R, and the other part is the anisotropic long-range moment, resulting from the polarization of one molecule by the quadrupole field of the other molecule, which varies as R^{-4}. The overlap induction effect contributes mainly to the intensity of the broad Q (i.e., Q_{overlap}) components ($\Delta J = 0$, J being the rotational quantum number).

The interesting feature of the Q branch in the collision-induced fundamental band of H_2 is the occurrence of the dips in the Q_{overlap} components. The low- and high-wave-number maxima of these dips are known as Q_P and Q_R, the separation of which is strongly density dependent. The quadrupolar induction effect contributes to the intensity of the relatively less broad O ($\Delta J = -2$), Q (i.e., Q_{quad}; $\Delta J = 0$, and S ($\Delta J = +2$) components.

The quadrupolar components in the induced fundamental band of a pure diatomic gas consists of single transitions $O_1(J)$, $Q_1(J)$ ($J \neq 0$), and $S_1(J)$ and double transitions of the types $Q_1(J) + Q_0(J)$ and $Q_1(J) + S_0(J)$.[7,8] In a single transition one of the colliding pair of molecules makes the vibrational or the vibrational-rotational transition while the internal energy of the other molecule does not change; in a double transition both the colliding molecules simultaneously absorb a photon which corresponds to a vibrational transition $Q_1(J)$ in one molecule and a rotational transition $S_0(J)$ or an orientational transition $Q_0(J)$ ($J \neq 0$) in the other molecule.

Considerable progress has been made to date in the analysis of the absorption profiles of the fundamental band of H_2 in the *pure gas* by Welsh and his collaborators.[9-12] It was shown that the absorption coefficient (see Sec. II) in the low- and high-wave-number wings of the Q branch obeys the *Boltzmann relation*

$$\tilde{\alpha}^-(\nu_m - \Delta\nu) = \tilde{\alpha}^+(\nu_m + \Delta\nu)\exp(-hc\Delta\nu/kT) \quad , \qquad (1)$$

where $\tilde{\alpha}^-(\nu_m - \Delta\nu)$ is the absorption coefficient (with the wave-number factor removed) at a wave number $\Delta\nu$ lower than the molecular wave number ν_m (in cm^{-1}) and $\tilde{\alpha}^+(\nu_m + \Delta\nu)$ is the absorption coefficient at a wave number $\Delta\nu$ higher than ν_m.[11] A similar relation was found to be valid for the S lines of the induced pure rotational spectrum of H_2.[13] Hunt and Welsh[10] analyzed most of the high-wave-number wing of the fundamental band of H_2 at 78, 195, and 300 K by representing the overlap Q_R component of the Q branch with a dispersion line form[13] and the quadrupolar S components by a Boltzmann-modified dispersion line form. Later Watanabe and Welsh[11] analyzed the absorption profiles of the band at low densities and low temperatures (18–77 K), where the dip in the Q branch was not very apparent, by representing both the overlap and the quadrupolar components by a Boltzmann-modified dispersion line form. Subsequent-

ly, Watanabe[12] analyzed the absorption profiles of the band at 18, 20.4, and 24 K by making use of the theoretical matrix elements of the quadrupole moment[14] and of the polarizability of H_2.[15]

The line shapes discussed above are empirical in nature and have no theoretical basis. As a matter of fact, in collision-induced absorption the line shape must be derived from the Fourier transform of the intercollisional time correlation function of the induced dipole moment. Levine and Birnbaum[16] in an attempt to obtain a theoretical line shape for the observed collision-induced pure translational spectra of the rare-gas mixtures[17] arising on account of the short-range overlap induced dipole moments used a Gaussian-type dipole moment which tends to zero as R tends to zero. Assuming ideal straight-line collision paths for the colliding molecules, Levine and Birnbaum[16] calculated an *intracollisional line shape* (i.e., relating to single collisions) in the form of a modified Bessel function of the second kind. Van Kranendonk[18] showed that the splitting in the overlap Q branch could be interpreted in terms of the negative correlations existing between the short-range dipole moments induced in successive collisions. This *intercollisional interference effect* is density dependent and the corresponding dip of the Q branch in the collision-induced fundamental band was shown by Van Kranendonk[18] to be represented by a dispersion-type intensity distribution. Recently, Mactaggart *et al.*[19,20] have analyzed satisfactorily the enhancement absorption profiles of the fundamental band of H_2 in several H_2-inert gas mixtures, which consist of single transitions, by using the Levine-Birnbaum line shape and Van Kranendonk's dispersion-type line shape for the intracollisional part and the intercollisional part, respectively, of the overlap-induced Q components and the dispersion line shape for the quadrupole-induced Q and S components.

In the present study the more complex structure of the absorption profiles of the collision-induced fundamental band of H_2 in the pure gas obtained at 77, 196, and 298 K was analyzed by using the recently derived new line shapes. The results of the analysis were used to determine the overlap parameters λ and ρ, which represent the magnitude and range, respectively, of the overlap dipole moment, and $\mu(\sigma)$, the overlap-induced dipole moment at the Lennard-Jones intermolecular diameter σ, for the H_2-H_2 collision pairs from the theory of Van Kranendonk.[6]

II. EXPERIMENTAL DETAILS

The absorption profiles of the fundamental band of H_2 in the pure gas were recorded for gas densities up to 60 amagat at liquid nitrogen (77 K) and dry-ice–acetone mixture (196 K) temperatures with a 2-m absorption cell and at room temperature (298 K) with a 1-m and the 2-m absorption cells constructed of stainless steel. These cells are of the transmission type and have been described in detail elsewhere.[21] The source of infrared radiation was a General Electric FFJ quartzline projection lamp housed in a water-cooled brass jacket. The spectrometer used was a Perkin-Elmer Model 112 single-beam double-pass instrument equipped with an LiF prism and an uncooled PbS detector. The original 13-Hz mechanical chopper in the spectrometer was replaced by a 260 Hz tuning fork chopper Model L-40 supplied by American Time Products. A Dunn Model LI-101 preamplifier and a Brower Laboratories Model 101 lock-in voltmeter were used in the detection-amplification system for the signal. A satisfactory reduction in the level of the atmospheric water-vapor absorption around 3800 and 5300 cm^{-1} in the background was achieved by flushing the entire optical path outside the absorption cell with dry nitrogen during the experiments. Mercury emission lines and absorption peaks of atmospheric water vapor were used for the wavenumber calibration. The slit width maintained at 35 μm gave a spectral resolution of ~3.0 cm^{-1} at the origin (4161 cm^{-1}) of the fundamental band.

The absorption coefficient $\alpha(\nu)$ at a given wave number ν(in cm^{-1}) of an absorbing gas at a density ρ_a is given by

$$\alpha(\nu) = (1/l)\ln[I_0(\nu)/I(\nu)] \quad , \tag{2}$$

where l is the sample path length of the absorption cell, and $I_0(\nu)$ and $I(\nu)$ are the intensities of radiation transmitted by the evacuated cell and by the cell filled with the absorbing gas, respectively. Absorption profiles were obtained by plotting $\log_{10}[I_0(\nu)/I(\nu)]$ against ν. The integrated absorption coefficients $\int \alpha(\nu)d\nu$ of the band were determined from the areas measured under the absorption profiles.

It was confirmed that there was no noticeable ortho-para conversion of the H_2 molecules in the stainless-steel cell at low temperature during an experiment, by monitoring the intensities of the $S_1(0)$ and $S_1(1)$ groups in an experiment at 77 K for a given density of the gas.

III. ABSORPTION PROFILES AND ABSORPTION COEFFICIENTS

Examples of absorption profiles recorded in the present study at 77, 196, and 298 K are shown as solid curves in Figs. 1, 2, and 3, respectively. The positions of the single transitions $O_1(J)$,

$Q_1(J)$, and $S_1(J)$ for the appropriate J values calculated from the constants of the free H_2 molecule[22] are marked along the wave-number axis. Almost all the H_2 molecules are distributed among the rotational states $J=0$ and 1 at 77 K and $J=0$ to 3 at 196 and 298 K. It is to be noted that for H_2 the even and odd J levels correspond to the para and ortho modifications, respectively. The occurrence of the dip in the Q branch at the position of the $Q_1(1)$ line (4155 cm^{-1}) of the free H_2 molecule and the effect of temperature on the profiles, as seen in Figs. 1–3, and the increase in the separation $\Delta\nu_{PR}^{max}$ between the Q_P and Q_R maxima with density of the gas are very well known from the previous work (see Ref. 9, for example).

The integrated absorption coefficients $\int \alpha(\nu)d\nu$ of the band can be expressed as a power series in terms of density ρ_a of the gas by the relation

$$\int \alpha(\nu)d\nu = \alpha_{1a}\rho_a^2 + \alpha_{2a}\rho_a^3 + \cdots , \qquad (3)$$

where α_{1a} (cm^{-2} $amagat^{-2}$) and α_{2a} (cm^{-2} $amagat^{-3}$) are the binary and ternary absorption coefficients, respectively. Plots of $(1/\rho_{H_2}^2)\int \alpha(\nu)d\nu$ against ρ_{H_2} for the three experimental temperatures are shown in Fig. 4 and are found to be straight lines. The values of the binary and ternary absorption coefficients obtained from, respectively, the intercepts and slopes of these lines which were determined by a least-squares fit of the experimental data are listed in Table I. The integrated absorption coefficients can also be represented by the

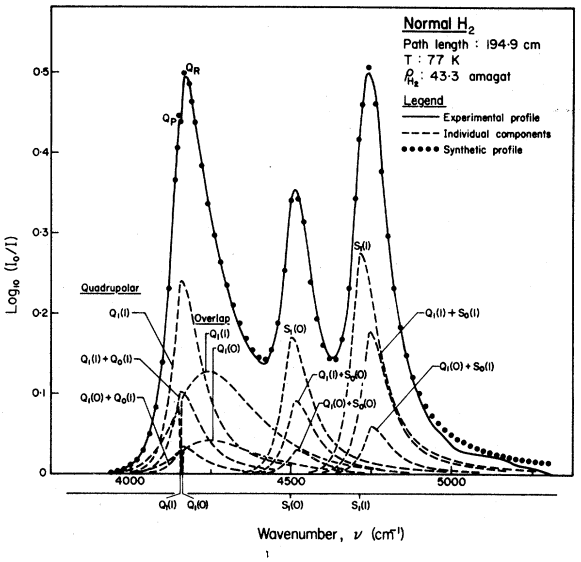

FIG. 1. Absorption profile of the collision-induced fundamental band of H_2 in the normal gas at a density of 43.3 amagat at 77 K. The solid curve is the experimental profile. The dashed curves represent two overlap-induced and nine quadrupole-induced computed components and the dots represent the summation of these. Note that the quadrupole-induced components $Q_1(0)$ and $Q_1(0)+Q_0(0)$ do not occur.

relation

$$c\int \tilde{\alpha}(\nu)d\nu = \tilde{\alpha}_{1a}\rho_a^2 n_0^2 + \tilde{\alpha}_{2a}\rho_a^3 n_0^3 + \cdots , \qquad (4)$$

where c is the speed of light, $\tilde{\alpha}(\nu)=\alpha(\nu)/\nu$, and n_0

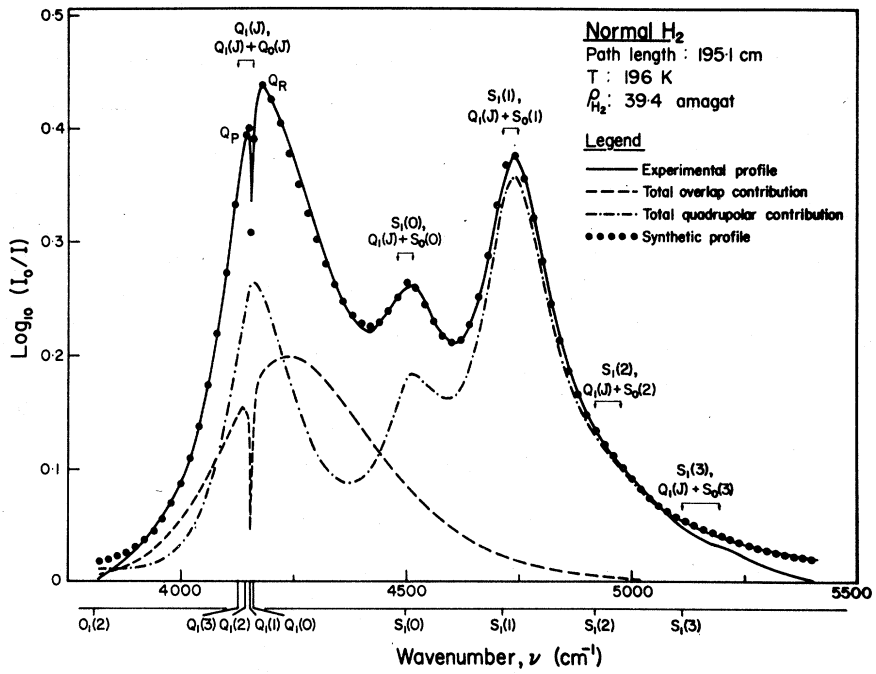

FIG. 2. Absorption profile of the collision-induced fundamental band of H_2 in the normal gas at a density of 39.4 amagat at 196 K. Here the rotational quantum number J takes the values 0 to 3. The solid curve is the experimental profile. The dashed curve represents the computed overlap-induced profile consisting of the components $Q_{1\,overlap}(J)$, $J=0$ to 3. The dot-dashed curve represents the computed quadrupole-induced profile consisting of the single transitions $O_1(J)$, $J=2$ and 3; $Q_1(J)$, $J=1$ to 3; $S_1(J)$, $J=0$ to 3; and double transitions $Q_1(J)+Q_0(J)$, $J=1$ to 3; and $Q_1(J)+S_0(J)$, $J=0$ to 3. The dots represent the sum of the computed overlap and quadrupolar components.

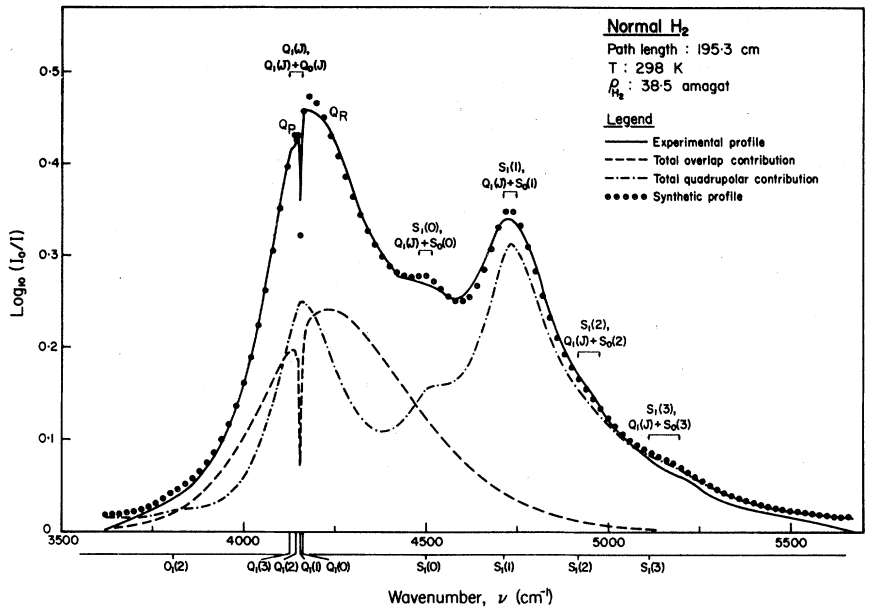

FIG. 3. Absorption profile of the collision-induced fundamental band of H_2 for a gas density of 38.5 amagat at 298 K. Refer to the caption of Fig. 2 for other details.

is the Loschmidt's number. The new binary and ternary absorption coefficients $\tilde{\alpha}_{1a}$ (cm^6 sec^{-1}) and $\tilde{\alpha}_{2a}$ (cm^9 sec^{-1}) are related to α_{1a} and α_{2a}, respectively, by the expressions

$$\tilde{\alpha}_{1a} = (c/n_0^2)\alpha_{1a}/\bar{\nu}, \quad \tilde{\alpha}_{2a} = (c/n_0^3)\alpha_{2a}/\bar{\nu} \ , \tag{5}$$

where the band center $\bar{\nu}$ is given by

$$\bar{\nu} = \int \alpha(\nu)d\nu \Big/ \int \alpha(\nu)\nu^{-1}d\nu \ . \tag{6}$$

The values of $\bar{\nu}$ at 77, 196, and 298 K are 4483, 4466, and 4444 cm^{-1}, respectively. The values of $\tilde{\alpha}_{1a}$ are also listed in Table I. Also included in the same table are the values of the absorption coefficients obtained by the previous investigators. The values of the coefficients obtained in the present work at 77 and 298 K compare very well with the corresponding values obtained previously. However, the values at 196 K are somewhat smaller than those obtained by Hunt.[23]

IV. ANALYSIS OF THE ABSORPTION PROFILES

An analysis of the absorption profiles was performed by fitting the calculated profile to the observed spectrum. In all, a total of 47 profiles were analyzed with a computer program. In this section, the line shapes used, the relative intensities of various transitions, the method of computation, and the results of the analysis will be described.

A. Line shapes

For the overlap-induced components, the absorption coefficient $\tilde{\alpha}(\nu)$ is given by the relation[18,19]

$$\tilde{\alpha}(\nu) = \frac{\tilde{\alpha}_{0m}^0 W_0^0(\Delta\nu)D(\Delta\nu)}{1+\exp(-hc\Delta\nu/kT)} \ , \tag{7}$$

where $\tilde{\alpha}_{0m}^0$ is the fictitious relative maximum intensity of an overlap-induced transition at the molecular wave number $\nu = \nu_m$ of the H_2 molecule. The quantity $W_0^0(\Delta\nu)$ with $\Delta\nu = \nu - \nu_m$ represents the intracollisional line form proposed by Levine and

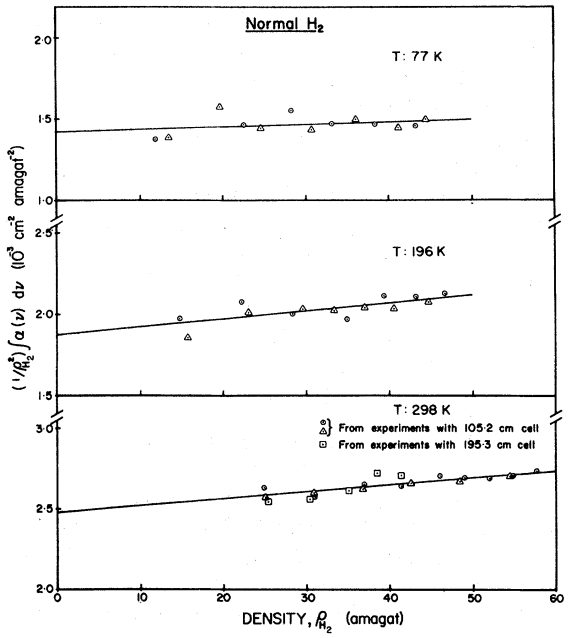

FIG. 4. Plots of $(1/\rho_{H_2}^2)\int \alpha(\nu)d\nu$ vs ρ_{H_2} at 77, 196, and 298 K.

TABLE I. Absorption coefficients[a] of the fundamental band of normal H_2 at 77, 196, and 298 K.

	Binary absorption coefficient		Ternary absorption coefficient	
T (K)	α_{1a} (10^{-3} cm^{-2} amagat^{-2})	$\tilde{\alpha}_{1a}$ (10^{-35} cm^6 sec^{-1})	α_{2a} (10^{-6} cm^{-2} amagat^{-3})	Reference
77	1.42 ± 0.05	1.32 ± 0.05	1.5 ± 1.5	Present work
	1.44	1.37		Hunt[b]
		1.32 ± 0.02		Watanabe and Welsh[c]
196	1.87 ± 0.05	1.74 ± 0.05	4.9 ± 1.3	Present work
	2.04	1.89		Hunt[b]
298	2.46 ± 0.03	2.30 ± 0.03	4.7 ± 0.7	Present work
	2.5		2.0	Chisholm and Welsh[d]
	2.4		1.1	Hare and Welsh[e]
	2.42	2.24		Hunt[b]

[a] Ranges of error indicated in the present work are standard deviations.
[b] Reference 23.
[c] Reference 24.
[d] Reference 9.
[e] Reference 25.

Birnbaum[16] and may be expressed as

$$W_0^0(\Delta\nu) = (2\Delta\nu/\delta_d)^2 K_2(2\Delta\nu/\delta_d) \ , \tag{8}$$

where K_2 is a modified Bessel function of the second kind and δ_d is the intracollisional half-width at half-height. The quantity $D(\Delta\nu)$ is the intercollisional line form which is given by Van Kranendonk[18] as

$$D(\Delta\nu) = 1 - \gamma[1 + (\Delta\nu/\delta_c)^2]^{-1} \ , \tag{9}$$

where γ is a constant which is assumed to be unity in the present analysis, and δ_c is the intercollisional half-width at half-height. In Eq. (7), the factor in the denominator converts the symmetrized line form into the observed Boltzmann-modified line form.

For the quadrupole-induced components, the absorption coefficient is represented by the Boltzmann-modified dispersion line form[13] which is given by

$$\tilde{\alpha}^+ = \frac{\tilde{\alpha}^0_{qm}}{1 + (\Delta\nu/\delta_q)^2} \ , \quad \Delta\nu \geq 0 \ , \tag{10}$$

$$\tilde{\alpha}^- = \tilde{\alpha}^+ \exp(-hc\Delta\nu/kT), \quad \Delta\nu < 0 \ , \tag{11}$$

where $\tilde{\alpha}^+$ and $\tilde{\alpha}^-$ are the absorption coefficients at wave numbers $\nu_m + \Delta\nu$ and $\nu_m - \Delta\nu$ in the high- and low-wave-number wings, respectively, $\tilde{\alpha}^0_{qm}$ is the relative maximum intensity of a quadrupole-induced component at $\nu = \nu_m$, and δ_q is the half-width at half-height, measured to the high-wave number wing. The profile analysis was repeated by using a "symmetrized" dispersion line shape[19] for the quadrupole-induced components which is represented as

$$\tilde{\alpha} = \frac{\tilde{\alpha}^0_{q',m}[1 + (\Delta\nu/\delta_{q'})^2]^{-1}}{1 + \exp(-hc\,\Delta\nu/kT)} \ , \tag{12}$$

where $\tilde{\alpha}^0_{q',m}$ is the relative maximum intensity and $\delta_{q'}$ is the half-width at half-height of the symmetrized dispersion line.

B. Relative intensities

The relative intensities of the overlap-induced components $Q_{1\,\mathrm{overlap}}(J)$ were calculated from the relation[6]

$$\tilde{\alpha}_{0m} = P_J \ , \tag{13}$$

where P_J is the Boltzmann factor for the rotational state J normalized in such a way that $\sum_J P_J = 1$ and is given by

$$P_J = (1/Z) g_T (2J+1) \exp(-E_J/kT) \ . \tag{14}$$

Here, Z is the rotational partition function $\sum_J g_T(2J+1)\exp(-E_J/kT)$ and $g_T = 1$ and 3 for the even and odd states J of H_2, respectively. Equation (14) holds for equilibrium hydrogen. For normal hydrogen

$$\sum_{\text{even } J} P_J : \sum_{\text{odd } J} P_J = 1:3 \ .$$

The relative intensities of the quadrupole-induced single transitions $O_1(J)$, $Q_1(J)$ $(J \neq 0)$, and $S_1(J)$ and the quadrupole-induced double transitions $Q_1(J) + Q_0(J)$ $(J \neq 0)$ and $Q_1(J) + S_0(J)$ are given in terms of the H_2 quadrupole moment and polarizability matrix elements $\langle vJ|Q_{H_2}|v'J'\rangle$ and $\langle vJ|\alpha_{H_2}|v'J'\rangle$ by the following relations:[26] For the single transitions

$$\tilde{\alpha}^0_{qm} = P_{J_1} P_{J_2} C(J_1 2 J_1'; 00)^2 C(J_2 0 J_2'; 00)^2 \times \langle 0 J_1 | Q_1 | v_1' J_1' \rangle^2 \langle 0 J_2 | \alpha_2 | v_2' J_2' \rangle^2 \ . \quad (15)$$

For the double transitions

$$\tilde{\alpha}^0_{qm} = P_{J_1} P_{J_2} C(J_2 2 J_2'; 00)^2 C(J_1 0 J_1'; 00)^2 \times \langle 0 J_2 | Q_2 | v_2' J_2' \rangle^2 \langle 0 J_1 | \alpha_1 | v_1' J_1' \rangle^2 \ . \quad (16)$$

Here, the subscripts 1 and 2 refer to the two colliding molecules, vJ and $v'J'$ are the initial and final vibrational and rotational quantum numbers, and $C(J\lambda J';00)$ with $\lambda = 0$ and 2 is a Clebsch-Gordan coefficient. For the fundamental band of H_2 one has $v_1' = 1$ and $v_2' = 0$, and the intensities of the single transitions are proportional to $\langle 0J|Q|1J'\rangle^2 \langle 0J|\alpha|0J\rangle^2$ and those of the double transitions are proportional to $\langle 0J|Q|0J'\rangle^2 \langle 0J|\alpha|1J\rangle^2$. The relative intensities of various quadrupolar transitions of the fundamental band of H_2 were calculated by theoretical matrix elements of the quadrupole moment and polarizability of the H_2 molecule, computed by Birnbaum and Poll[27] and Poll,[26] respectively. Finally, the relative intensities of the overlap and quadrupolar components were expressed, respectively, in terms of intensity of the $Q_{1\,\mathrm{overlap}}(1)$ component and the $S_1(1)$ component.

C. Method of computation and results of profile analysis

Analysis of the profiles of the enhancement of absorption was carried out by a program written for the IBM 370/155 computer. The two relative peak intensities of the overlap and quadrupolar components and their half-widths δ_d, δ_c, and δ_q (or $\delta_{q'}$), defined by Eqs. (8), (9), and (10) [or (12)], respectively, were the adjustable parameters in the program. Provision was also made in the computer program to adjust the molecular wave numbers ν_m of the quadrupolar H_2 lines in order to account for any possible perturbations of the H_2 vibrational wave numbers. A series of computations was carried out by the computer for different values of the adjustable parameters until the computed profile, which was the sum of the intensities of the individual transitions, gave the best nonlinear least-squares fit to the experimental profile in the entire region of the band. The computation thus provided the half-width parameters δ_d and δ_c of the overlap-induced components and δ_q and $\delta_{q'}$ of the quadrupole-induced lines. For the best fit of the computed profiles to the observed profiles, the computer also gave the overlap and quadrupolar contributions to the intensity of the band separately. An example of the results of the analysis for an absorption profile of the H_2 fundamental band at 77 K by using the Boltzmann-modified dispersion line shape for the quadrupolar lines is shown in Fig. 1. As the individual components contributing to the intensity of the band are only 11 at 77 K, these are shown separately in this figure. As can be seen from this figure, the agreement between the experimental and synthetic profiles is very good over the entire region of the band. Results of similar profile analysis for the H_2 fundamental band at 196 and 298 K are shown in Figs. 2 and 3. As the number of individual components at these temperatures are too many these are not shown separately in these figures; however, the total overlap and quadrupolar contributions are shown separately. An analysis performed with a symmetrized line shape for the quadrupole-induced lines gave equally good agreement between the observed and computed profiles at all the three temperatures. In all cases the best fit of the calculated profiles to the observed profiles was obtained for unshifted molecular wave numbers.

The results of the profile analysis are presented in Table II. It is seen from this table that the overlap contribution increases from 23% to 38% as the temperature increases from 77 to 298 K; equivalently, the quadrupolar contribution decreases from 77% at 77 K to 62% at 298 K. Within the range of densities used in the present experiments, δ_d, δ_q, and $\delta_{q'}$ are found to be independent of density at each of the temperatures. Figure 5 gives a plot of the average values of δ_d, δ_q, and $\delta_{q'}$ against $\sqrt{T}$, the square root of absolute temperature. The half-width parameter δ_d which varies

TABLE II. Results of profile analysis for normal H_2 gas.

T (K)	Intracollisional half-width δ_d (cm^{-1})	Collision duration[a] τ_d (10^{-14} sec)	Quadrupolar half-width δ_q (cm^{-1})	Collision duration[b] τ_q (10^{-14} sec)	Symmetrized quadrupolar half-width $\delta_{q'}$ (cm^{-1})	Overlap contribution (%)	Quadrupolar contribution (%)
77	192 ± 5	2.8	74 ± 2	7.2	53 ± 1	23	77
196	211 ± 6	2.5	112 ± 2	4.7	86 ± 1	31	69
298	248 ± 3	2.1	135 ± 2	3.9	107 ± 2	38	62

[a] $\tau_d = 1/2\pi c \delta_d$.
[b] $\tau_q = 1/2\pi c \delta_q$.

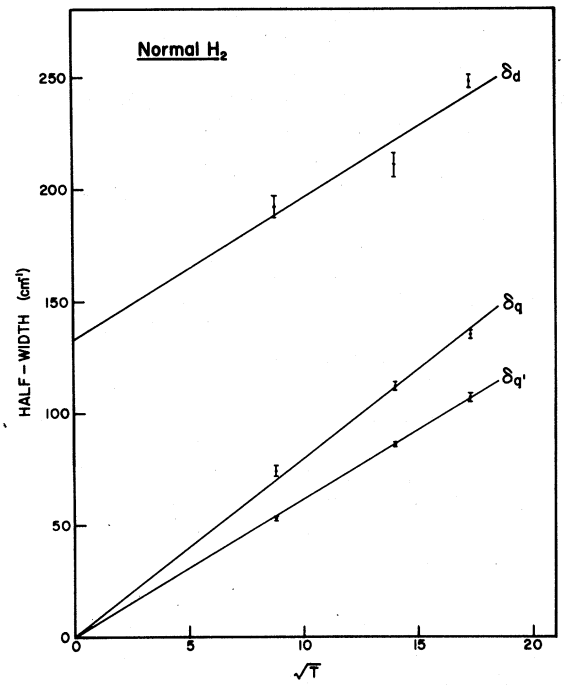

FIG. 5. Half-widths δ_d, δ_q, and $\delta_{q'}$ vs the square root of the absolute temperature T.

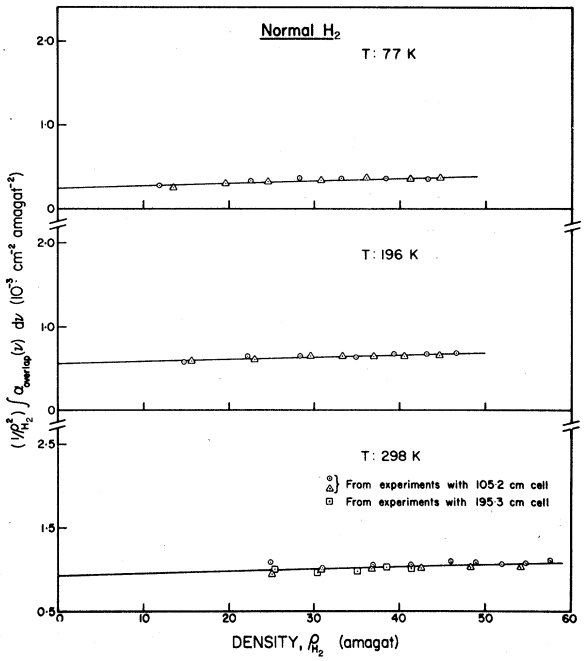

FIG. 6. Plots of $(1/\rho_{H_2}^2)\int \alpha_{\text{overlap}}(\nu)d\nu$ obtained from the profile analysis vs ρ_{H_2} at 77, 196, and 298 K.

linearly with $\sqrt{T}$, when extrapolated to $T=0$ has a value of 133 cm^{-1}, which indicates that even at $T=0$ the duration of collision $\tau_d(=1/2\pi c\delta_d)$ is still relatively short because the overlap induction occurs mainly in the region of the strong repulsive forces (see also Ref. 19). The quadrupolar half-widths δ_q and $\delta_{q'}$ are found to satisfy the linear relations $\delta_q = 7.97\sqrt{T}$ and $\delta_{q'} = 6.16\sqrt{T}$. The intercollisional half-width δ_c increases with increasing density of the H_2 gas. As the present experiments with pure H_2 gas were limited to densities up to 60 amagat only, it was not possible to derive a definite expression for the density dependence of δ_c. The values of δ_c for the maximum experimental densities of the gas at 77, 196, and 298 K were less than 0.4, 3.0, and 3.5 cm^{-1}, respectively. In order to obtain a reliable density-dependent relation for δ_c experiments must be extended to higher densities.

V. OVERLAP PARAMETERS FOR THE H_2 - H_2 COLLISION PAIRS

The integrated overlap absorption coefficients $\int \alpha_{\text{overlap}}(\nu)d\nu$ derived in Sec. IV from the profile analysis can be represented by a relation which is similar to Eq. (3)

$$\int \alpha_{\text{overlap}}(\nu)d\nu = \alpha_{1a\text{overlap}}\rho_a^2 + \alpha_{2a\text{overlap}}\rho_a^3 + \cdots \quad . \tag{17}$$

Plots of $(1/\rho_{H_2}^2)\int \alpha_{1a\text{overlap}}(\nu)d\nu$ vs ρ_{H_2} are shown in Fig. 6 and are found to be straight lines. The overlap binary and ternary absorption coefficients $\alpha_{1a\text{overlap}}$ ($cm^{-2}\,amagat^{-2}$) and $\alpha_{2a\text{overlap}}$ ($cm^{-2}\,amagat^{-3}$) were obtained, respectively, from the intercepts and slopes of these lines, which were calculated from the linear least-squares fits. The values of these coefficients and of $\tilde{\alpha}_{1a\text{overlap}}$ ($cm^6\,sec^{-1}$) calculated from the relation

$$\tilde{\alpha}_{1a\text{overlap}} = (c/n_0^2)\alpha_{1a\text{overlap}}/\bar{\nu} \quad , \tag{18}$$

$\bar{\nu}$ being the center of the overlap profile [cf. Eq. (5)], are listed in Table III.

According to Van Kranendonk,[6] the binary absorption coefficient $\tilde{\alpha}_{1a\text{overlap}}$ can be represented by the relation

$$\tilde{\alpha}_{1a\text{overlap}} = \lambda^2 I\tilde{\gamma} \quad , \tag{19}$$

where the dimensionless quantity λ is related to $M_0(R)$, the rate of change of the overlap-induced dipole moment μ_{overlap} with respect to the internuclear separation r at its equilibrium value $r=r_0$, by the relation

$$M_0(R) = \xi \exp(-R/\rho) = \lambda e \exp[-(R-\sigma)/\rho] \quad , \tag{20}$$

[or $\lambda = (\xi/e)\exp(-\sigma/\rho)$]. Here λe is the amplitude of the oscillating overlap-induced dipole moment when the intermolecular separation R becomes σ corresponding to the Lennard-Jones potential $V(\sigma)=0$. The overlap-induced dipole moment $\mu(R)$ at

TABLE III. Absorption coefficients [a] of the overlap part of the fundamental band of normal H_2 at three different temperatures.

T (K)	Binary absorption coefficient $\alpha_{1a\ \text{overlap}}$ (10^{-3} cm^{-2} amagat^{-2})	Binary absorption coefficient $\tilde{\alpha}_{1a\ \text{overlap}}$ (10^{-35} cm^6 sec^{-1})	Ternary absorption coefficient $\alpha_{2a\ \text{overlap}}$ (10^{-6} cm^{-2} amagat^{-3})
77	0.25 ± 0.02	0.24 ± 0.02	3.0 ± 0.5
196	0.56 ± 0.02	0.54 ± 0.02	2.5 ± 0.5
298	0.93 ± 0.04	0.90 ± 0.04	2.6 ± 0.8

[a] Ranges of error indicated are standard deviations.

$R = \sigma$ is given by $\mu(\sigma) = \lambda e \sigma$. The parameters ξ and ρ give, respectively, the magnitude and range of the overlap-induced dipole moment. In Eq. (19), the temperature-dependent dimensionless integral $I(T^*)$, where $T^* = kT/\epsilon$ is given by

$$I(T^*) = 4\pi \int_0^\infty \exp[-2(x-1)(\sigma/\rho)] g_0(x) x^2 dx \ , \quad (21)$$

where $x = R/\sigma$, and $g_0(x)$ is the low-density limit of the pair-distribution function and is equal to $\exp[-V^*(x)/T^*]$ classically with $V^*(x) = V(x)/\epsilon$, $V(x)$ being the Lennard-Jones potential $V(x) = 4\epsilon(x^{-12} - x^{-6})$. The quantity $\tilde{\gamma}$ in Eq. (19) which has the dimensions of the binary absorption coefficient is given by

$$\tilde{\gamma} = (8\pi^3/3h) e^2 \sigma^3 \kappa_1^2 \ , \quad (22)$$

where κ_1, in the matrix notation, is represented as $\langle 0|(r - r_0)|1\rangle$. The value of $\tilde{\gamma}$ calculated by making use of the theoretical matrix element $\langle vJ|(r - r_0)|v'J'\rangle$ with $v = 0$, $J = 0$, $v' = 1$, $J' = 0$, calculated by Poll[28] is 5.60×10^{-32} cm^6 sec^{-1}. The values of σ(= 2.928 Å) and ϵ/k(= 37.00) were taken from Ref. 29.

A plot of $\lambda^2 I$ obtained from the values of $\tilde{\alpha}_{1a\text{overlap}}$ and $\tilde{\gamma}$ [cf. Eq. (19)] vs temperature T is shown in Fig. 7. The integral I depends on σ/ρ [cf. Eq. (21)] and the most probable value of σ/ρ for the H_2-H_2 pairs was determined by a procedure similar to the one used by Reddy and Chang.[3] The details are as follows: The values of I were computed for a series of values ρ/σ in the range 0.070–0.140 at intervals of 0.002 at reduced temperatures T^* in the range 0.5–20.0 at intervals of 0.5. Appropriate values of I were obtained either directly or extrapolated from the data given by Van Kranendonk and Kiss.[30] For a particular value of σ/ρ, λ^2 which is assumed to be independent of temperature was calculated from the value of $\lambda^2 I$ at one of the temperatures from the corresponding value of I. The values of $\lambda^2 I$ at the other two experimental temperatures were in turn calculated and compared with the corresponding experimental values. This procedure was repeated for a series of values of σ/ρ until the calculated values of $\lambda^2 I$ at the three temperatures agreed closely with the corresponding experimental values.

The criterion used for the best fit of the curve $\lambda^2 I$ vs T was that $\sum_i \delta_i^2$ be a minimum, where δ_i are the deviations of the calculated values of $\lambda^2 I$ from the corresponding experimental values. The calculated values of $\lambda^2 I$ for the best fit are also shown in Fig. 7. The values of ρ/σ and λ for H_2-H_2 obtained from the best fit are given in Table IV. Also included in the table are the values of ρ, σ, and $\mu(\sigma)$ (the overlap-induced dipole moment corresponding to the Lennard-Jones diameter σ). Hunt[23] obtained a value of 0.126 for ρ/σ for the H_2-H_2 molecular pairs, which is about one and a

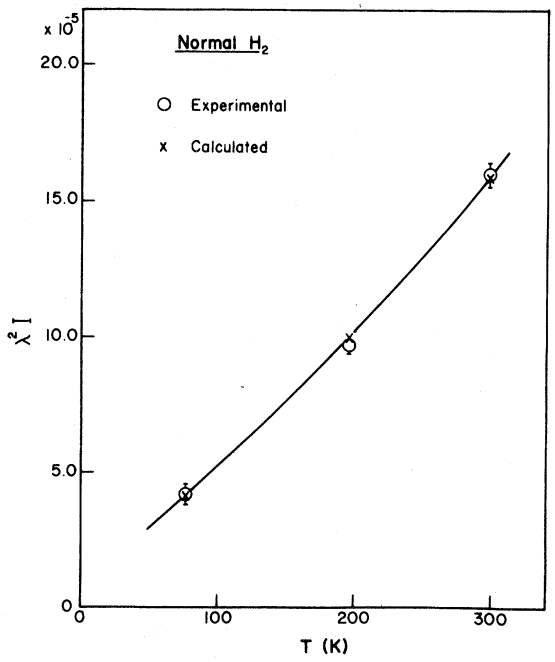

FIG. 7. Variation of $\lambda^2 I$ with the absolute temperature T.

half times higher than the value obtained in the present work. The higher value of ρ/σ obtained by Hunt may be understood on the basis of the following reasons: (i) The Q branch splitting which is rather a dominant feature of the absorption profiles at higher temperatures has been ignored and only the high-frequency wing of the band has been analyzed; (ii) the double-transition quadrupolar components $Q_1(J) + Q_0(J)$ of the Q branch as well as several double transition lines of the S branch have also been neglected; and (iii) the new theoretical line shapes proposed by Levine and Birnbaum[16] and Van Kranendonk[18] were not available at the time of that analysis.

VI. CONCLUDING REMARKS

In principle, the absolute intensities of the quadrupole-induced lines arising from binary collisions can be calculated from the theoretical expressions (see, for example, Poll[26]). In the case of mixtures of H_2 with inert gases Poll *et al.*[31] pointed out that a considerable part of the intensity of the so-called quadrupolar S lines comes from the anisotropic overlap contribution which was neglected in the original "exponential-4" model for the induced dipole moment.[6]

Recently, McKellar *et al.*[32] found that the value of the calculated binary absorption coefficient of the quadrupolar components for the case of the H_2 fundamental band in H_2-He mixtures agrees with the value obtained from the profile analysis in which it was assumed that the anisotropic overlap interaction contributes to the intensity of the S lines of the band. In the present work on the fundamental band of H_2 in the pure gas the theoretical value of the binary absorption coefficient of the quadrupolar $S_1(1)$ line at 77 K is found to be 0.36 $\times 10^{-7}$ cm^{-1}amagat^{-2}, whereas the corresponding experimental value is $(0.53 \pm 0.01) \times 10^{-7}$ cm^{-1}amagat^{-2}. The experimental value was obtained from the profile analysis where a Boltzmann-modified dispersion line form was used for the quadrupole-induced lines with the assumption that the intensities of the O and S lines were completely due to the quadrupolar induction. One must note that the calculated values of the binary absorption coefficient of the quadrupole-induced lines are very sensitive to small uncertainties in the value of the Lennard-Jones diameter σ of the colliding pair of molecules, which occurs in the *fifth power* in the theoretical expressions.[26] A simple calculation shows that a 7% decrease in the value of σ is necessary to account for this large difference of ~47% in the theoretical and experimental values of the binary absorption coefficient. Therefore, it is possible that a part of the difference between the calculated and experimental values of the binary absorption coefficients of the S lines may arise from the *anisotropic overlap* contribution.[31]

TABLE IV. Overlap parameters for the H_2-H_2 molecular pairs.

ρ/σ	λ	σ (Å)	ρ (Å)	$\mu(\sigma)$ ($10^{-2}\, ea_0$)
0.080	4.53×10^{-3}	2.928	0.23	2.5

ACKNOWLEDGMENT

We are grateful to Professor J. D. Poll for helpful discussions and for making available to us the theoretical values of the matrix elements $\langle vJ|(r - r_0)|v'J'\rangle$ of the hydrogen molecule prior to publication.

†Work supported in part by a grant awarded to SPR from the National Research Council of Canada.

*On leave from the University of Zambia, Lusaka, Zambia.

‡Holder of a Graduate Fellowship of the Memorial University of Newfoundland, 1972–75.

[1]H. L. Welsh, M. F. Crawford, and J. L. Locke, Phys. Rev. 76, 580 (1949).

[2]H. L. Welsh, MTP *International Review of Science, Physical Chemistry, Vol. 3, Spectroscopy,* edited by D. A. Ramsay (Butterworths, London, 1972), and the references therein.

[3]S. P. Reddy and K. S. Chang, J. Mol. Spectrosc. 47, 22 (1973) and the references therein.

[4]A. R. W. McKellar, J. W. Mactaggart, and H. L. Welsh, Can. J. Phys. 53, 2060 (1975) and the references therein.

[5]J. Van Kranendonk, Physica 23, 825 (1957).

[6]J. Van Kranendonk, Physica 24, 347 (1958).

[7]The subscripts 0 and 1 attached to O, Q, and S refer to the change in the vibrational quatum number v.

[8]If the anisotropy of the polarizability of the molecules is considered double transitions of the type $S_1(J) + S_0(J)$ could occur. However, these were found to be too weak to be observed in the present spectra.

[9]D. A. Chisholm and H. L. Welsh, Can. J. Phys. 32, 291 (1954).

[10]J. L. Hunt and H. L. Welsh, Can. J. Phys. 42, 873 (1964).

[11]A. Watanabe and H. L. Welsh, Can. J. Phys. 45, 2859 (1967).

[12]A. Watanabe, Can. J. Phys. 49, 1320 (1971).

[13]Z. Kiss and H. L. Welsh, Can. J. Phys. 37, 1249 (1959).
[14]G. Karl and J. D. Poll, J. Chem. Phys. 46, 2944 (1967).
[15]W. Kolos and L. Wolniewicz, J. Chem. Phys. 46, 1426 (1967).
[16]H. B. Levine and G. Birnbaum, Phys. Rev. 154, 86 (1967).
[17]D. R. Bosomworth and H. P. Gush, Can. J. Phys. 43, 729 (1965).
[18]J. Van Kranendonk, Can. J. Phys. 46, 1173 (1968).
[19]J. W. Mactaggart and H. L. Welsh, Can. J. Phys. 51, 158 (1973).
[20]J. W. Mactaggart, J. De Remigis, and H. L. Welsh, Can. J. Phys. 51, 1971 (1973).
[21]R. D. G. Prasad, Ph.D. thesis (Memorial University of Newfoundland, 1976) (unpublished).
[22]B. P. Stoicheff, Can. J. Phys. 35, 730 (1957).
[23]J. L. Hunt, Ph.D. thesis (University of Toronto, 1959) (unpublished).
[24]A. Watanabe and H. L. Welsh, Can. J. Phys. 43, 818 (1965).
[25]W. F. J. Hare and H. L. Welsh, Can. J. Phys. 36, 88 (1958).
[26]J. D. Poll, in *Proceedings I.A.U. Symposium 40 on Planetary Atmospheres* (Reidel, Dordrecht, Holland, 1971), p. 384.
[27]A. Birnbaum and J. D. Poll, J. Atmos. Sci. 26, 943 (1969).
[28]J. D. Poll (private communication).
[29]J. O. Hirshfelder, C. F. Curtiss, and R. B. Bird, *Molecular Theory of Gases and Liquids*, 2nd ed. (Wiley, New York, 1967).
[30]J. Van Kranendonk and Z. J. Kiss, Can. J. Phys. 37, 1187 (1959).
[31]J. D. Poll, J. L. Hunt, and J. W. Mactaggart, Can. J. Phys. 53, 954 (1975).
[32]A. R. W. McKellar, J. W. Mactaggart, and H. L. Welsh, Can. J. Phys. 53, 2060 (1975).